THE GENERATION OF PHYSICAL STRUCTURE IN POWER AND REFRIGERATION SYSTEMS

A. Bejan

J. A. Jones Professor of Mechanical Engineering, Duke University, Durham, NC 27708-0300, USA

ABSTRACT

This paper presents a broad view of the 'constructal' principle that accounts for the generation of structure and performance improvements in power and refrigeration systems. Such systems owe their thermodynamic imperfection to a multitude of internal and external flows (heat, fluid, electricity) that must overcome resistances. Designs are destined to remain imperfect, because resistances are reflections of the global constraints that are imposed (e.g., finite size, weight, cost). Resistances compete against each other. They must be optimized together, and balanced against each other. In this way the thermodynamic imperfection (irreversibility) is distributed in near-optimal ways (more uniformly) through the system, such that the global performance level is maximized. Optimal distribution means structure, configuration, flow topology, and design. The generation of structure in the pursuit of optimal global performance subject to global constraints is illustrated by means of several class-wide examples: the optimal distribution of heat exchanger inventory in a power plant, the optimal distribution of intermediate cooling along the thermal insulation structure of a low-temperature refrigerator or liquifier, the optimal intermittent (on-off) operation of ice-making processes, defrosting refrigerators and power plants with periodically cleaned heat exchangers, and the optimal cruising speed for powered flight (airplanes, birds, insects).

KEYWORDS : Constructal, optimization, topology, design, geometric form, rhythm, intermittent operation, flight

1. CONSTRUCTAL DESIGN AND THEORY

The engineering thermodynamics literature of the last two decades reflects the important changes that have taken place in methodology in the wake of the renewed interest triggered by the energy crisis. The methods of exergy analysis, entropy generation minimization (EGM) and thermoeconomics are the most established manifestations of these changes. In this paper I review an even more recent development in the method of thermodynamic optimization, namely, the construction of the system: the generation of the physical structure (topology) of the engineered system, as a result of global optimization subject to finite-resources constraints [1].

The objective of the method of thermodynamic optimization is to identify the ways (features, procedures) by which the system fulfills its functions while performing at the highest thermodynamic level possible [2-22]. We seek designs that operate least irreversibly. Designs are destined to remain imperfect, because finite-size constraints such as specified heat transfer surfaces will always force currents (e.g., heat, fluid) to flow against resistances. The challenge then is to do the 'best possible' under the specified constraints. This is accomplished by spreading the imperfections through the system in optimal ways. Optimal spreading constitutes the generation of physical structure—the actual being of the engineered system.

Optimal distribution of imperfection is the principle that generates topology (construction, configuration) in flow systems. It was shown that this 'constructal' principle [1] generates morphology not only in engineered flow systems but also in naturally occurring flow systems. The thought that the constructal principle is a law of physics that accounts for the generation of flow structure everywhere is 'constructal theory'.

2. ALLOCATION OF HEAT EXCHANGERS

We start with the system that triggered the industrial revolution and the science of thermodynamics: the heat engine. The system is closed and operates steadily, or in an integral number of cycles, between two fixed temperatures, high (T_H) and low (T_L). Its purpose is to convert the specified heat input (Q_H, fixed) into mechanical power (W), Figure 1. The lateral boundaries of the system are insulated perfectly such that heat is forced to flow vertically. Better performance means more W for the same unit of Q_H.

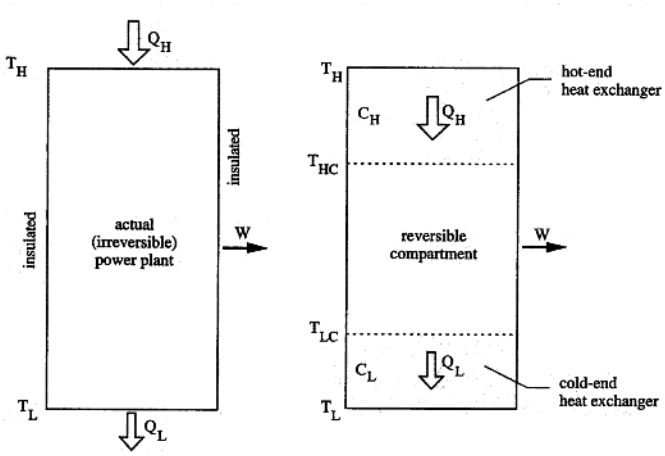

Figure 1 Model of irreversible power plant with hot-end and cold-end heat exchangers.

Irreversible operation is a characteristic of real power plants, and a reflection of the physical constraints (e.g. finite sizes) that designs must face. Consequently, the energy conversion ratio W/Q_H is expectedly lower than the Carnot efficiency, $W/Q_H < 1 - T_L/T_H$. A simple way to illustrate the origin of the inequality sign is to recognize that the heat input Q_H and the rejected heat Q_L are driven in the indicated directions by *finite* temperature differences [2-5]. These differences are located inside the power plant, as shown on the right side of Figure 1. One way to account for the relationship between heat transfer rate and temperature difference is to assume the proportionalities $Q_H = C_H(T_H - T_{HC})$ and $Q_L = C_L(T_{LC} - T_L)$, where the conductances are $C_H = (UA)_H$ and $C_L = (UA)_L$, with A for heat transfer surface, and U for overall heat transfer coefficient based as A. Each thermal conductance is proportional to the size of the heat exchanger surface. When U_H and U_L are of the same order of magnitude, it makes sense to regard C_H and C_L as partners in an overall size constraint [4]

$$C_H + C_L = C, \quad \text{constant} \tag{1}$$

It is assumed that the rest of the power plant—the compartment shown between T_{HC} and T_{LC} in Figure 1—operates reversibly. This means that the rate of entropy generation in this compartment is zero. Combining the second law statement $Q_L/T_{LC} - Q_H/T_{HC} = 0$ with the first law for the same compartment ($W = Q_H - Q_L$), we arrive at the energy conversion ratio of the power plant, $W/Q_H = 1 - T_{LC}/T_{HC}$. This ratio is smaller than its Carnot limit, because $T_{HC} < T_H$ and $T_{LC} > T_L$. The W/Q_H ratio may be rewritten to show explicitly the effect of distributing the C inventory to the two heat exchangers,

$$\frac{W}{Q_H} = 1 - \frac{T_H}{T_L}\left[1 - \frac{Q_H}{T_H C}\left(\frac{1}{x} + \frac{1}{1-x}\right)\right]^{-1} \tag{2}$$

In this expression $x = C_H/C$ is the conductance allocation fraction, such that $C_L/C = 1 - x$. It is evident that when C_H and C_L vary subject to the size constraint (1) the power output and conversion ratio are maximized when $x = 1/2$, i.e. when $C_H = C_L$.

To take the given hardware (C), to cut it into two pieces of special sizes (C_H, C_L), and to install these pieces in special places in the system means to endow the system with *structure*. The maximization of the global performance (2) pinpointed the optimal configuration, $C_H = C_L$. Global optimization subject to size constraint generated structure. The engineering literature continues to show that $C_H = C_L$ holds at least approximately for increasingly complex models of irreversible power plants, and for the corresponding class of models of irreversible refrigeration plants [4, 23].

Hand in hand with the balancing and minimization of resistances to internal flow, comes the requirement to guide each current along a certain path. In a power plant the heat input must be forced to flow through the machine, in order to do the most work possible, because otherwise it would leak directly into the ambient, bypassing the machine. The guiding of the heat current is achieved through the distribution of *insulation*, in configurations where the insulated surfaces are nonisothermal. The examples shown in Refs. [1, 24] illustrate how a finite amount of material can be distributed optimally (unevenly), and that the maximization of global insulation effect lends geometric form to the design.

3. STRUCTURE IN LOW TEMPERATURE MACHINES

The field of refrigeration engineering is rich in examples of structures generated by the purpose and constraints principle. The purpose of a refrigerating machine is to maintain a cold space cold. The space cannot remain cold by itself because of the leakage of heat from the ambient. No insulation is perfect. Furthermore, in most applications the heat leak is only one of the heat currents that threaten the cold space: additional examples are the heat currents due to electrical resistances, friction between moving parts, and the movement of warm materials into the cold space and cold materials out of the cold space (e.g., domestic refrigerators, helium liquefiers).

The heat currents that reach the cold space must be "forced" to flow in the unnatural direction, toward room temperature. This requires work, or power. The purpose of the machine is not only to maintain the low temperature of the cold space, but to do so with least power expenditure. To do something is not enough. To do it better and better, in spite of the constraints, is the real objective, the drive.

The origin of geometric structure in the objective and constraints principle can be illustrated on the basis of the simplest possible model of a refrigerating machine [2, 4, 23]. The cold-space temperature is T_L and the ambient temperature is T_H. The only heat current that reaches the cold space is due to the leakage through the insulation of cross-sectional area A, thickness L and effective thermal conductivity k. These parameters (T_L, T_H, A, L, k) are fixed and play the role of constraints in the discussion that follows. For simplicity we also assume that the effective thermal conductivity is independent of temperature, so that for the configuration shown in the upper part of Figure 2 we write $Q_0 = (k\ A/L)\ (T_H - T_L)$. In this configuration the current Q_0 is conserved as it flows from T_H to T_L; this current must be removed as Q_0 from T_L.

We assume that this task is accomplished by a reversible refrigerating machine, which in the steady state requires the power input

$$W_0 = Q_0\left(\frac{T_H}{T_L} - 1\right) \tag{3}$$

The direction for improvements is indicated by Eq. (3). The power requirement W_0 is large because the temperature ratio T_H/T_L is large (T_L is small). The machine will use less power if its cold end is attached to the insulation at an intermediate temperature T_m, which is larger than T_L. This method is tried in the lower part of Figure 2. Now the insulation has structure: two layers,

each with its own constant heat current, Q_H and Q_L. The position of the cooled plane (T_m) is indicated by the dimensionless parameter x, which is defined by the thickness (xL) of the layer of insulation between T_m and T_L. Both T_m and x are variable. The T_m refrigerator removes the heat current difference $Q_H - Q_L$, requiring the power

$$W_m = (Q_H - Q_0)\cdot\left(\frac{T_H}{T_m} - 1\right) \tag{4}$$

where $Q_H = kA(T_H - T_m)/[(1 - x)L]$ and $Q_L = kA(T_m - T_L)/(xL)$. There is still a need for refrigeration at T_L, because the heat current Q_L reaches the cold space. The power required by the T_L refrigerator is

$$W_L = Q_L\left(\frac{T_H}{T_L} - 1\right) \tag{5}$$

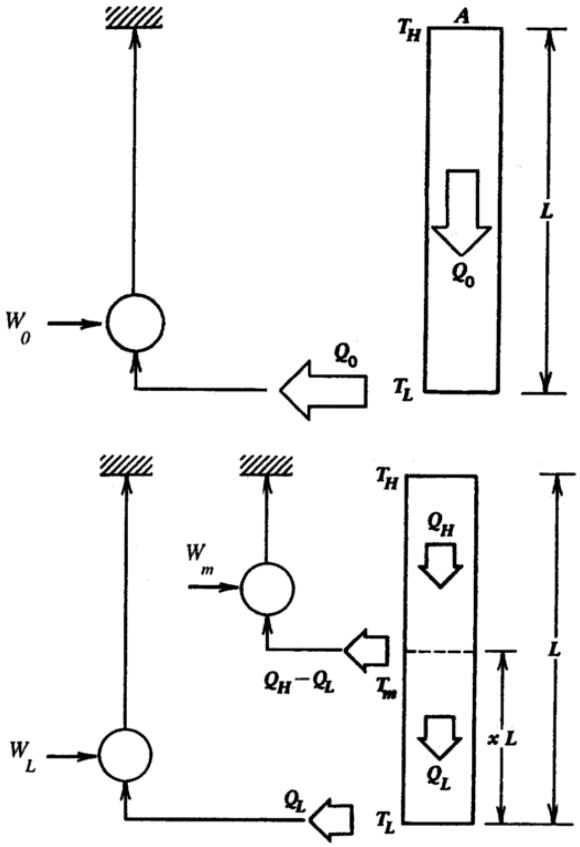

Figure 2 Insulation with cold-end cooling (top), and with intermediate and cold-end cooling (bottom).

Important is the sum of the two power requirements ($W_m + W_L$), which can be expressed in a form that shows the effect of varying x and T_m. It can be shown [1] that by minimizing this expression we arrive at geometric structure (x_{opt}) and thermal structure ($T_{m,opt}$):

$$x_{opt} = \frac{1}{2} \qquad T_{m,opt} = (T_L T_H)^{1/2} \tag{6}$$

The goodness of this structure relative to the reference design shown in the upper part of Figure 2 is measured by the ratio $(W_m + W_L)_{min} / W_0$. It is found that this ratio decreases when T_L decreases [1]. In conclusion, the structure revealed in the lower part of Figure 2 is especially recommended for low temperature systems.

The intermediate cooling example that we just completed is the start of an extensive body of work that has generated complex structures for low temperature refrigerating machines. The idea of cooling the insulation at an intermediate temperature in a given interval ($T_H - T_L$ in Figure 2), is valid for any other interval. Immediate candidates are the sections $T_H - T_m$ and $T_m - T_L$. After this optimization, the L-thick insulation acquires a more complex structure (four layers), which is sustained by intermediate cooling applied at three locations, in addition to the T_L end. This optimization can be repeated several times until the intermediate cooling is distributed almost continuously along the insulation, from T_H to T_L. The optimal design for this limit is located based on variational calculus subject to fixed geometry (A/L) [4, 23]. The conclusion is that the optimal heat current varies *continuously* through the insulation, $Q_{opt}(T)$.

Structure is the engineer's way of implementing this result. Uniform cooling can be provided by a stream of cold gas flowing from T_L to T_H in counterflow with the heat leak (Q_H, Q_L) shown in Figure 2. The capacity rate of this stream has a special value, which is pinpointed by $dQ_{opt}/dT = (\dot{m}c_p)_{opt}$. The design and fabrication of the heat transfer surface between the stream and the insulation are difficult. When the insulation is a solid structural member, bringing the stream in close thermal contact with the solid means to weaken the solid by machining channels in it. An alternative is to approximate the uniform cooling scheme by building heat exchangers at a few locations.

There are many other types of insulation that lend themselves to the intermediate cooling technique. A stack of concentric radiation shields built around the cold space works in the same way as the one-dimensional insulation (k, A, L) discussed until now. The role of A is played by the shield surface (the cross-section of the radiation heat leak), the role of L is played by the number of shields, and the effective k depends on temperature because it accounts for the temperatures and radiative properties of mutually facing surfaces. Electrical current leads and power cables, which are necessary in superconducting systems, must also be cooled continuously [1, 4].

It is convincing that all these structures are commonplace in cryogenic engineering practice, and that they have their origin in a single principle: the con structal principle of objective and constraints. Now a unifying view accounts for the seemingly diverse and unrelated structures developed independently by engineers over many decades, in separate schools, design rooms, countries and continents. If we look at all these forms strictly from the point of view of today, assuming no knowledge of their historical development and the principle that generated them, we are struck by their combination of diversity, similarities and continuity (persistence, survival). We are struck in the same way as when we admire the many living species and the many river basins. Engineering design opens our

eyes to the principle that generates diversity, similarities and continuity throughout nature—the inanimate, the animate and the engineered.

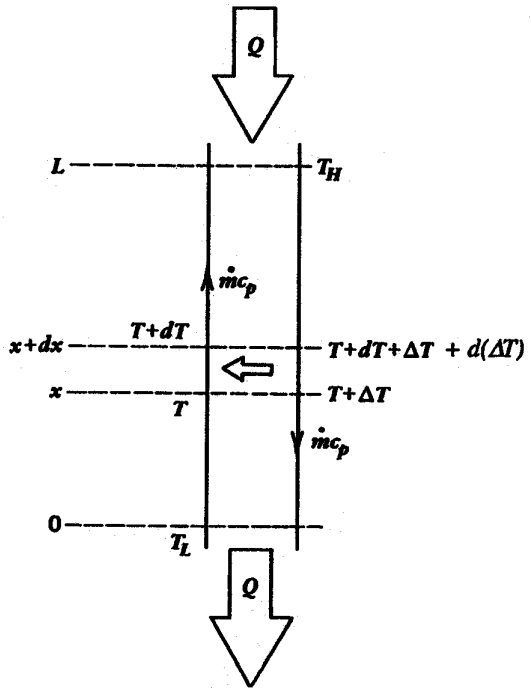

Figure 3 Counterflow heat exchanger, where the enhancement of thermal contact in the stream-to-stream direction is equivalent to increasing the insulation effect in the end-to-end direction.

4. COUNTERFLOWS

Even more prevalent in machines is the counterflow heat exchanger cooled along its length. The cold structure of every low temperature refrigerator and liquefier is dominated by a vertical counterflow heat exchanger, which brings warm and compressed gas down to the coldest space, and returns low-pressure gas up to room temperature. The two streams are in intimate thermal contact: the descending stream is cooled by the rising stream (Figure 3). The large heat transfer area (A) between the two streams is responsible for the small but finite local temperature difference ΔT. Ideal gas behavior is assumed on both sides of the heat exchanger. Invoking the first law for one of the streams, we obtain $\dot{m}c_p dT = U\Delta T dA$. In this expression U is the overall stream-to-stream heat transfer coefficient based on A. The constraint is the contact area, which is obtained by integrating the preceding expression.

The area size constraint confirms the known rule that small stream-to-stream temperature differences require a large con tact area. Less known about counterflows is this: excellent stream-to-stream thermal contact means excellent insulation in the end-to-end direction. This alternative view holds that the counterflow is a path for net energy transfer in the longitudinal direction, i.e. an insulation system. The energy that flows is the convective heat current Q in dicated by the vertical arrows in Figure 3. The magnitude of Q is the difference between the enthalpy of the descending stream $\left[\dot{m}c_p(T+\Delta T)\right]$ that crosses the plane x, and the enthalpy of the ascending stream $(\dot{m}c_p T)$, namely, $Q=\dot{m}c_p\Delta T$. In a 1979 paper [25, 26] I showed that the longitudinal heat current emerges is a quantity proportional to the longitudinal temperature gradient, where p is the contact area per unit length of stream flow, p = dA/dx,

$$Q = \frac{(\dot{m}c_p)^2}{Up}\frac{dT}{dx} \qquad (7)$$

The proportionality between the convective heat current and the longitudinal temperature gradient is analogous to the Fourier law for heat conduction. Consequently, every structural feature that was derived for the unidirectional insulation exhibited in Figure 2 also holds for the column (control volume) that houses the counterflow. The intermediate cooling effect must be distributed uniformly along L, that is, along the temperature span $T_L - T_H$. This can be accomplished by using an additional stream of cold gas $(\dot{m}_e)$ is placed in counterflow with the convective heat current Q. It can be made available by bleeding an optimal fraction of the warm high-pressure stream and expanding it through a work producing device (cylinder and piston, or turbine). The analysis is presented in detail in Refs. [25, 26], although it can be reproduced based on the preceding relations. The optimal flow imbalance is $\dot{m}_{e,opt}/m = (\dot{m}c_p/UA)\ln(T_H/T_L)$.

Together, the three streams constitute a counterflow heat exchanger with slightly unbalanced capacity rates, where the cold side $(\dot{m}+\dot{m}_e)$ is larger than the warm side. The optimal imbalance derived above is reflected in a tapering of the temperature gap between the two streams, such that the smaller temperature differences are near the cold end. This smooth taper can be produced when the cold stream is delivered by a single expander, i.e., when the pressure ratio P_H/P_L is large enough so that the expander embraces the entire temp-erature scale of the heat exchanger, $T_H - T_L$. When the temperature span of one expander is too small relative to $T_H - T_L$, the tapering of the ΔT or more expanders along the main heat exchanger. There is an analogy between the use of a few expanders and the use of a few intermediate cooling stations along a con-ducting support. Furthermore, the physical structure of optimally distributed expanders can be observed in practically every machine built for operation at liquid nitrogen temperature (77 K) and liquid helium temperature (4.2 K). They were not built based on the theory reviewed in this paper and in Ref. [1]. The theory came much later. Existing engineering structures, with their great diversity and striking similarities, call for a unifying form-generating principle as much as all the natural structures.

Nature offers many examples of structures with streams in counterflow. For these, natural scientists have offered the same purpose-based explanation as the design principle for engineered counterflows: Natural streams are organized in counterflow in order to reduce the convective current (heat, or mass species) that flows

longitudinally. Best known is the example of the blood counterflow in the long legs of wading birds, and in whale flippers [27-29]. The body of the bird is warm, and the foot is cold, in the water. Warm oxygenated blood flows downward and is cooled in counterflow by the returning venous blood. In this way the loss of body heat through the foot is minimized. Otherwise, the body extension (foot) would act as any other extended surface and maximize the loss of body heat. Numerous other counterflows prevent the excessive loss of water from animals living in the desert [29].

In biomedical engineering, the longitudinal convective heat transfer expression (13) was rediscovered in 1985 by Weinbaum and Jiji [30]. This effect was incorporated in a heat transfer model of the vascularized tissue, to account for the occurrence of countercurrent pairs of thermally significant blood vessels. In this model Eq. (13) makes an additional, convective contribution to the effect of conduction through the living tissue.

In a paper that was just published [31], I showed that two balanced tree-shaped flows in founterflow, one warmer than the other, constitute a single tree-shaped flow of convective currents. The tree counterflow structure is common in the vascularized tissue under the skin of a warm blooded animal. The total heat current convected (leaked) by the double tree is proortional to the total tree volume raised to the power ¾. This is the first purely theoretical derivation of the universally observed proportionality between metabolic rate and body mass raised to the power ¾, in all animals.

All these natural counterflows are structures with purpose. The great geometric and functional similarities between the naturally occurring structures and the engineered ones strengthen the view that the constructal principle makes sense in rationalizing the occurrence of structure in every compartment of nature, inanimate systems, animate systems, and engineered systems.

5. POWERED FLIGHT

More evidence that what generates form in engineering also generates form in nature comes from the study of powered flight. As in refrigeration and other power consuming systems, our theoretical starting point is the objective—to do the most based on the power or fuel consumed. The flying structure that is generated by this principle has many features. More obvious are the shapes: bodies, wings, feathers and flaps. More hidden are the internal parts such as the hollow bones of birds and the aluminum parts of most airplanes. Even more subtle is the speed of the flying body, on which we focus in this section.

The most basic features and needs of powered flight are retained in the upper-right detail of Figure 4. The flying body of mass M has the linear dimension D, density ρ_b, and horizontal speed V relative to the surrounding air. The air density ρ_a is much smaller than ρ_b. This leads to the global requirement that the net vertical body force $Mg \sim \rho_b D^3 g$ must be supported by other forces. The generation of the latter is achieved through the relative motion called flight.

By accounting for the conservation of mass and momentum in the control volume occupied by the flying body and the immediately close fluid regions affected by relative motion, it was shown that the power required to increase the kinetic energy of the air stream, from the inlet to the outlet, $\dot{W} \sim (1/2)\dot{m}\left(V_{out}^2 - V^2\right)$, is

$$\dot{W} \sim \frac{\rho_b^2 g^2 D^4}{\rho_a V} + \rho_a D^2 V^3 \tag{8}$$

This two-term expression shows the power that is required to maintain the body in the air (the first term), and to overcome the drag (the second term). The power function (8) has a minimum with respect to V,

$$V_{opt} \sim 3^{-1/4} \left(\frac{\rho_b}{\rho_a} gD\right)^{1/2} \tag{9}$$

Astonishingly good agreement exists between the principle-generated flying speed formula and the flying speeds found in nature and engineering [32, 33]. Since the body length scale D is the same as $(M/\rho_b)^{1/3}$, the optimal speed of Eq. (9) is proportional to the body mass raised to the power 1/6,

$$V_{opt} \sim \frac{\rho_b^{1/3} g^{1/2}}{\rho_a^{1/2}} M^{1/6} \tag{10}$$

Figure 4 shows that the flying speeds of all the things we know align themselves on a power-law curve of the predicted type. The data are from a more extensive compilation, from many independent sources [33]. The agreement between the predicted and the observed is not only qualitative but also quantitative. All flying animals and machines are represented by the orders of magnitude $\rho_b \sim 10^3$ kg/m^3 and $\rho_a \sim 1$ kg/m^3 (air at atmospheric conditions). The V_{opt} formula (10) becomes, roughly

$$V_{opt} \sim 30 (M/\text{kg})^{1/6} \text{ m/s} \tag{11}$$

which has been drawn on Figure 4. We see how the minimization of power consumption or exergy destruction unites all the flying systems, the animate with the engineered.

What we accomplished based on simple thermodynamic optimization in this section is only a sketch, a hint. The *complete* thermomechanical analysis of the flying body, and the geometric optimization of the internal and external architecture, will establish exactly what fraction of the used food or fuel is needed to produce the exergy $(\dot{W})$ needed to sustain the flight.

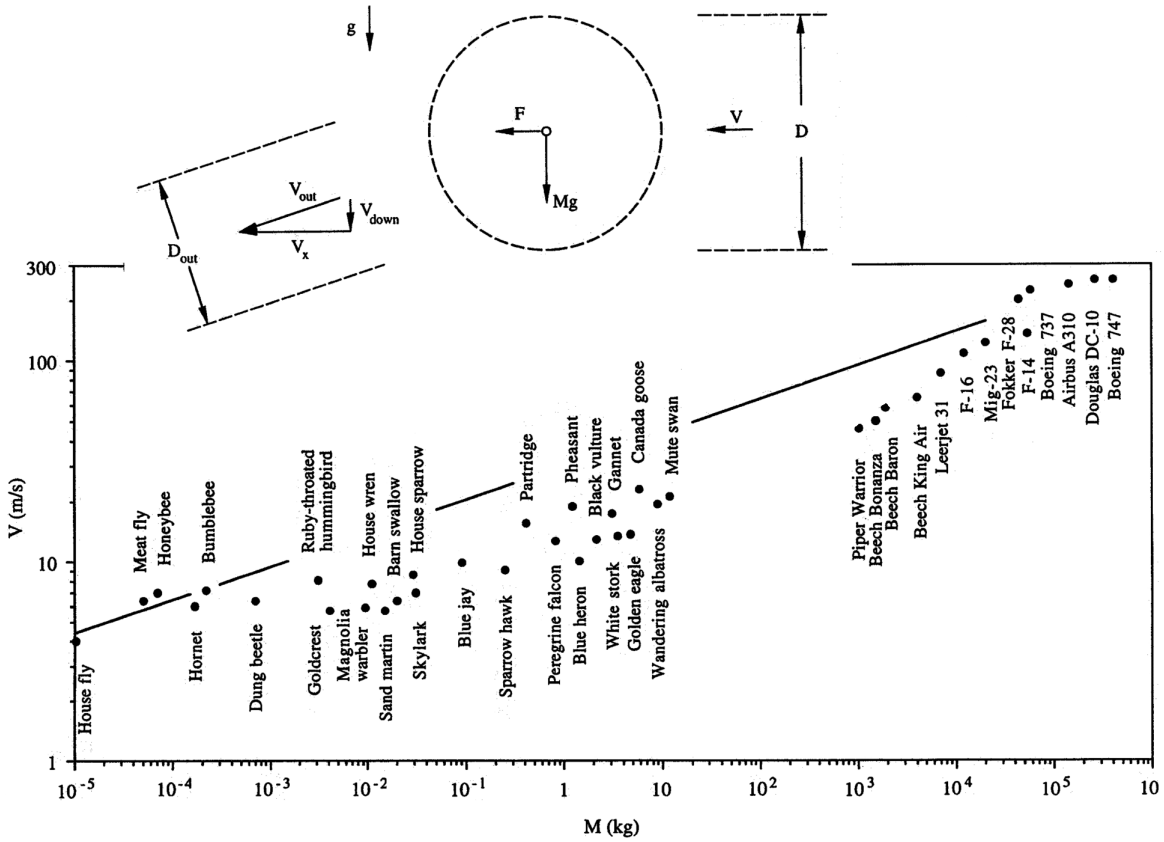

Figure 4 Simple model and interactions of a flying body, and the cruising speeds of insects, birds and airplanes [1].

6. RHYTHM

Nature impresses us not only with structure in space but also with structure in time—rhythm, or characteristic periodicity. The same holds for many engineering systems. Best known among the natural flows that exhibit rhythm are the breathing and heart beating of all animals. These intermittent flows are the basis for some of the most puzzling allometric laws, for example, the observed proportionality between frequency and animal body mass raised to the power of approximately –0.25. An elephant breaths less frequently than the mouse, and the human heart beats faster than the heart of the cow. The volume of theoretical material published on pulsating physiological processes is staggering. The preferred approach has been to take pulsating flows as given, i.e. not to question why nature has opted for periodic flow and not for steady flow. What has not been rationalized until recently [1] is the existence of finely tuned pulsating flows in nature.

Breathing and heart beating have a lot in common with engineered processes that are governed by time-dependent transport by diffusion. When we manufacture ice by freezing water on a cooled surface, the rate of ice formation decreases as the ice layer thickens. To maximize the time-averaged rate of ice production, we must terminate the freezing process, scrape the surface clean, and start over. To show that an optimal freezing time exists, it is a good idea to use the simplest freezing model possible. We assume therefore that the ice layer is sufficiently thin relative to the radius of curvature of the wall so that the wall may be regarded as plane (Figure 5). Water at the freezing point T_m is held in a channel the wall of which is suddenly cooled to a lower temperature, T_w, starting with the time $t = 0$. An ice layer grows on the cooled wall until the time $t = t_1$, when the cooling is interrupted, and the ice is removed. The time interval required to remove the ice, t_2, is assumed constant and known. This freezing and ice removal cycle of total duration $(t_1 + t_2)$ is repeated many times.

The thickness of the ice layer at the end of the freezing interval is $\delta_1 = b t_1^{1/2}$, where the constant b is shorthand for $[2k(T_m - T_w)/\rho\, h_{sf}]^{1/2}$. This solution is exact when the Stefan number $c(T_m - T_w)/h_{sf}$ is smaller than 1. The properties ρ, c and k are the density, specific heat and thermal conductivity of ice. The evolution of the ice thickness $\delta(t)$ and the freezing-removal production cycle are shown qualitatively in Figure 5. The objective is to maximize the amount of ice produced over the entire duration of one cycle, namely,

$$\bar{\delta} = \frac{\delta_1}{t_1 + t_2} = \frac{b}{t_2^{1/2}} \frac{\tau^{1/2}}{\tau + 1} \qquad (12)$$

The lone degree of freedom is the freezing time t_1, or its dimensionless counterpart $\tau = t_1/t_2$. By solving $d\bar{\delta}/d\tau = 0$ we find that $\tau_{opt} = 1$, or $t_{1,opt} = t_2$. The opti mal freezing time interval of the cycle is as long as the ice

removal interval. This conclusion changes somewhat as we include in the model additional features such as the wall curvature (e.g. freezing inside a tube), the finite heat transfer coefficient between the coolant and the outer surface of the water container, and the dependence between the ice removal time and the final thickness of the ice layer.

The essential point made by this simple analysis is that an optimal time of heat transfer exists, and that as a first approximation that time is equal to the time required to remove the ice layer. Furthermore, this conclusion is fundamental: an optimal freezing time exists in any installation (or more realistic model) for ice making based on freezing and contact melting. This optimization principle is relevant to the production by contact solidification of other solid materials, not just ice.

Optimized intermittent operation is a characteristic of many other engineered systems, some very complicated. Frost and ice grow on the evaporator surface of a refrigerator. An automatically defrosting refrigerator interrupts its cooling cycle and cleans the evaporator surface by melting the ice [34]. Power plants are shut down periodically so that the layers of dirt (scale, fouling) are scraped off the surfaces of their heat exchangers. Additional manifestations of this principle are found in the optimal operating lifetime of power plants driven by energy extracted from hot-dry-rock deposits [4]. The rock layers cool down by time-dependent diffusion, as the working fluid of the power plant is circulated through man made fissures. All these techniques are made necessary by the pursuit of objectives subject to constraints: they all generate structure in time.

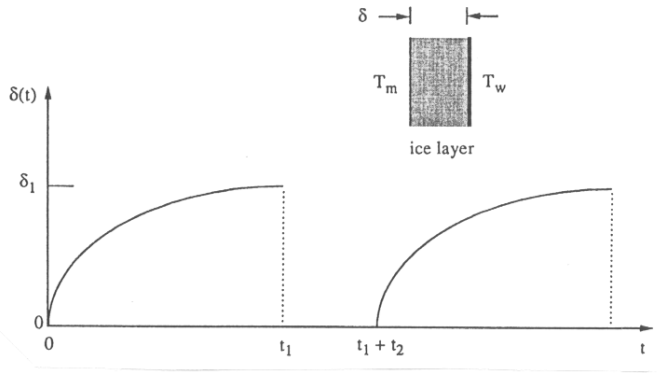

Figure 5 The intermittent production of ice: the freezing time τ_1, followed by the ice removal time τ_2.

7. CONCLUSION: STRUCTURE IS THE RESULT OF PRINCIPLE

The many examples—entire classes of applications—reviewed in this paper are united by the conclusion that the pursuit of objective subject to finite-resources constraints generates structure. Objective and constraints endow the flow system with geometry, architecture, rhythm.

In the engineering of flow systems the search for better global performance subject to present-day constraints is known as thermodynamic optimization, irreversibility minimization, or entropy generation minimization. Irreversibility is caused by currents that flow against resistances. There are many resistances (types, sizes), and they must be minimized together. The optimal balancing of the regions with different resistances (flow regimes) means that the material and channels must be distributed in certain ways. Better global performance is achieved when the distribution is relatively uniform, this, in spite of the gaping differences between the high- and the low-resistivity domains.

Optimal distribution of imperfection is the principle that generates form. The system is destined to remain imperfect. The system works best when its imperfection (its internal flow resistances) is spread around, so that more and more of the internal points are stressed as much as the constructal principle demands: objective served better, while under the grip of global and local constraints. There is a time arrow to all these forms, and it points toward the better.

The many and diverse manifestations of the constructal principle are reviewed in a new book [1].

REFERENCES

[1] Bejan, A., *Shape and Structure, from Engineering to Nature*, Cambridge University Press, Cambridge, UK, ISBN 0 521 79049 2 (2000).

[2] Feidt, M., *Thermodynamique et Optimisation Énergetique des Systèmes et Procedés,* Technique et Documentation, Lavoisier, Paris, ISBN 2743000589 (1996).

[3] Moran, M. J., *Availability Analysis: A Guide to Efficient Energy Use*, Prentice-Hall, Englewood Cliffs, ISBN 0 791 80009 1 (1989).

[4] Bejan, A., *Entropy Generation Minimization*, CRC Press, Boca Raton, ISBN 0 8493 9651 4 (1996).

[5] Feidt, M. L., Thermodynamics and the optimization of reverse cycle machines, *Thermodynamic Optimization of Complex Energy Systems*, Bejan, A. and Mamut, E., eds., Dordrecht, The Netherlands, Kluwer Academic Publishers, pp. 385-402 (1998).

[6] Kotas, T. J., *The Exergy Method of Thermal Plant Analysis*, Krieger, Melbourne, Florida (1995).

[7] Moran, M. J. and Shapiro, H. N., *Fundamentals of Engineering Thermodynamics*, 3rd ed., New York, Wiley (1995).

[8] Radcenco, V., *Generalized Thermodynamics*, Bucharest, Editura Technica (1994).

[9] Evans, R. B., A proof that exergy is the only consistent measure of potential work (for chemical systems), PhD Thesis, Dartmouth College, Hanover, New Hampshire (1969).

[10] Reistad, G. M., Availability: concepts and applications, PhD Thesis, University of Wisconsin, Madison (1970).

[11] Sciubba, E., Optimisation of turbomachinery components by constrained minimisation of the local entropy production rate, Chapter in Bejan,

A. and Mamut, E. eds., *Thermodynamic Optimization of Complex Energy Systems*, Dordrecht, The Netherlands, Kluwer Academic Publishers (1999).

[12] Sciubba, E., Allocation of finite energetic resources via an exergetic costing method, Chapter in Bejan, A. and Mamut, E., eds., *Thermodynamic Optimization of Complex Energy Systems*, Dordrecht, The Netherlands, Kluwer Academic Publishers, pp. 151-162 (1999).

[13] Sciubba, E. and Melli, R., *Artificial Intelligence in Thermal Systems Design: Concepts and Applications*, New York, Nova Science (1998).

[14] Benelmir, E., Evans, R. B. and Von Spakovsky, M. R., High degree decentralization for the optimum thermoeconomic design of a combined cycle, *Int. J. Energy Environment Economics*, Vol. 2, pp. 155-164 (1992).

[15] Benelmir, R., Lallemand, M., Lallemand, A. and Von Spakovsky, M. R., Exergetic and economic optimization of a heat pump cycle, *Int. J. Energy Environment Economics*, Vol. 5, pp. 135-149 (1997).

[16] De Vos, A., *Endoreversible Thermodynamics of Solar Energy Conversion*, Oxford, UK, Oxford University Press (1992).

[17] Shiner, J. S., ed., *Entropy and Entropy Generation*, Dordrecht, Kluwer Academic Publishers (1996).

[18] Tsatsaronis, G., Design optimization using exergoeconomics, Chapter in Bejan, A. and Mamut, E., eds., *Thermodynamic Optimization of Complex Energy Systems*, Dordrecht, The Netherlands, Kluwer Academic Publishers, pp. 101-116 (1999).

[19] Valero, L. A., Correas, L. and Serra L., On-line thermoeconomic diagnosis of thermal power plants, Chapter in Bejan, A. and Mamut, E., eds., *Thermodynamic Optimization of Complex Energy Systems*, Dordrecht, The Netherlands, Kluwer Academic Publishers, pp. 117-136 (1999).

[20] Von Spakovsky, M. R. and Frangopoulos, C. A., The environomic analysis and optimization of a gas turbine cycle with cogeneration, *Thermodynamics and the Design, Analysis and Improvement of Energy Systems*, Vol. AES 33, ASME New York (1994).

[21] Olsommer, B., Favrat, D. and Von Spakovsky, M. R., An approach for the time-dependent thermoeconomic modeling and optimization of energy system synthesis, design and operation (Part I: Methodology and results), *Int. J. Appl. Thermodynamics*, Vol. 2, pp. 97-114 (1999).

[22] Olsommer, B., Favrat, D. and Von Spakovsky, M. R., An approach for the time-dependent thermoeconomic modeling and optimization of energy system synthesis, design and operation (Part II: Reliability and availability), *Int. J. Appl. Thermodynamics*, Vol. 2, pp. 177-186 (1999).

[23] Bejan, A., *Advanced Engineering Thermodynamics*, second ed., Wiley, New York, ISBN 0 471 14880 6 (1997).

[24] Bejan, A., *Heat Transfer*, Wiley, New York, ISBN 0 471 50290 1 (1993).

[25] Bejan, A., A general variational principle for thermal insulation system design, *Int. J. Heat Mass Transfer*, Vol. 22, pp. 219-228 (1979).

[26] Bejan, A., *Entropy Generation through Heat and Fluid Flow*, Wiley, New York, ISBN 0 471 09438 2 (1982).

[27] Schmidt-Nielsen, K., *How Animals Work*, Cambridge Univ. Press, Cambridge, UK, ISBN 0 521 08417 2 (1972).

[28] Vogel, S., *Life's Devices*, Princeton Univ. Press, Princeton, NJ, ISBN 0 691 02418 9 (1988).

[29] Schmidt-Nielsen, K., *Desert Animals: Physiological Problems of Heat and Water*, Oxford Univ. Press, Oxford, UK, ISBN 0 486 23850 4 (1979).

[30] Weinbaum, S. and Jiji, L. M., A new simplified bioheat equation for the effect of blood flow on the local average tissue temperature, *J. Biomech. Eng.*, Vol. 107, pp. 131-139 (1985).

[31] Bejan, A., The tree of convective heat streams: its thermal insulation function and the predicted ¾-power relation between body heat loss and body size, *Int. J. Heat Mass Transfer*, Vol. 44, pp. 699-704 (2001).

[32] Pennycuick, C. J., *Animal Flight*, Edward Arnold, London, UK, ISBN 0 713 12355 9 (1972).

[33] Tennekes, H., *The Simple Science of Flight: from Insects to Jumbo Jets*, MIT Press, Cambridge, MA, ISBN 0 262 20105 4 (1997).

[34] Bejan, A., Vargas, J. V. C. and Lim, J. S., When to defrost a refrigerator, and when to remove the scale from the heat exchanger of a power plant, *Int. J. Heat Mass Transfer*, Vol. 37, pp. 523-532 (1994).